Natural Products Discovery Hot Paper

DOI: 10.1002/ange.201306549

Crowdsourcing Natural Products Discovery to Access Uncharted Dimensions of Fungal Metabolite Diversity**

Lin Du, Andrew J. Robles, Jarrod B. King, Douglas R. Powell, Andrew N. Miller, Susan L. Mooberry, and Robert H. Cichewicz**

Abstract: *A fundamental component for success in drug discovery is the ability to assemble and screen compounds that encompass a broad swath of biologically relevant chemical-diversity space. Achieving this goal in a natural-products-based setting requires access to a wide range of biologically diverse specimens. For this reason, we introduced a crowdsourcing program in which citizen scientists furnish soil samples from which new microbial isolates are procured. Illustrating the strength of this approach, we obtained a unique fungal metabolite, maximiscin, from a crowdsourced Alaskan soil sample. Maximiscin, which exhibits a putative combination of polyketide synthase (PKS), non-ribosomal peptide synthetase (NRPS), and shikimate pathway components, was identified as an inhibitor of UACC-62 melanoma cells ($LC50 = 0.93\ \mu M$). The metabolite also exhibited efficacy in a xenograft mouse model. These results underscore the value of building cooperative relationships between research teams and citizen scientists to enrich drug discovery efforts.*

Fungi are a remarkable source of novel secondary metabolites, many of which have been developed for clinical applications.[1] Despite increasing interest in fungal secondary metabolites,[2] it is estimated that less than 7% of the >1.5 million species of fungi have been subjected to an investigation of their bioactive constituents.[3] It is reasonable to postulate that a significant number of compounds with potential therapeutic relevance await discovery from the largely untapped majority of fungal species.

During the last four years, our research group has prepared a collection of several thousand fungal isolates originating from three environmentally disparate regions: Alaska (arctic/sub-arctic), Hawaii (tropical), and Oklahoma (subtropical/semi-arid). Our collection efforts have been supplemented through a crowdsourcing program in which "citizen scientists" are invited to submit soil samples from their personal properties.[4] Crowdsourcing is emerging as an important tool for engaging the public in the scientific process, thereby enabling research teams to analyze, as well as access critical information and/or specimens that would otherwise remain inaccessible to scientific investigation. Crowdsourcing approaches have been used to address a wide variety of scientific questions/problems, including the distribution pattern of volcanic ash from Grímsvötn,[5a] the analysis of historic weather data,[5b] classifying newly discovered galaxies,[5c] mapping emergency medical equipment,[5d] and other applications.[5e]

Extracts from a majority of the fungal isolates incorporated into our collection have been screened by LC-MS and/or subjected to a panel of bioassays (cancer cell cytotoxicity, antibacterial, antifungal, and inhibition of fungal biofilm formation), resulting in the isolation of several intriguing compounds.[6] Recently, through our group's crowdsourcing initiative, we identified a *Tolypocladium* sp. isolate (based on ITS sequence data and morphological features) that was highly responsive to a range of culture manipulation strategies (Figure 1). Initially, an extract prepared from the fungus grown in potato dextrose broth (PDB) ($10\ g\,L^{-1}$ dried mashed potato, $5\ g\,L^{-1}$ glucose, $2\ g\,L^{-1}$ $NaNO_3$) showed the presence of two 15-residue peptides, efrapeptins F (**5**) and G (**6**; Figure 1a,e). When treated with the epigenetic modifier 5-azacytidine (DNA methylation inhibitor, 100 μM; Figure 1b,b′), co-cultured with *Pseudomonas fulva* (Fig-

[*] Dr. L. Du,[+] J. B. King, Dr. D. R. Powell, Prof. Dr. R. H. Cichewicz
Department of Chemistry and Biochemistry, Stephenson Life Sciences Research Center, University of Oklahoma
101 Stephenson Parkway Norman, OK 73019-5251 (USA)
E-mail: rhcichewicz@ou.edu
A. J. Robles,[+] Prof. Dr. S. L. Mooberry
Department of Pharmacology, University of Texas Health Science Center at San Antonio, 7703 Floyd Curl Drive
San Antonio, TX 78229 (USA)
E-mail: mooberry@uthscsa.edu
Prof. Dr. A. N. Miller
Illinois Natural History Survey, University of Illinois (USA)
Dr. L. Du,[+] J. B. King, Prof. Dr. R. H. Cichewicz
Natural Products Discovery Group and Institute for Natural Products Applications and Research Technologies, University of Oklahoma (USA)
Prof. Dr. S. L. Mooberry
Cancer Therapy & Research Center and Department of Medicine, University of Texas Health Science Center at San Antonio (USA)
[+] These authors contributed equally to this work.

[**] Research reported in this publication was supported by the National Institute of General Medical Sciences of the National Institutes of Health RO1GM092219 (R.H.C.), the President's Council Excellence Award (S.L.M.), and with support from the CTRC P30 Cancer Center Support Grant (CA054174) and the Flow Cytometry Shared Resource (S.L.M.). The X-ray diffractometer was purchased through a grant from the NSF (CHE-0130835). The LC-MS instrument used for this project was provided in part by a Challenge Grant from the Office of the Vice President for Research, University of Oklahoma, Norman Campus and an award through the Shimadzu Equipment Grant Program (R.H.C.). We gratefully acknowledge Ms. A. Reyor for supplying the soil sample used in this study.

Supporting information for this article is available on the WWW under http://dx.doi.org/10.1002/anie.201306549.

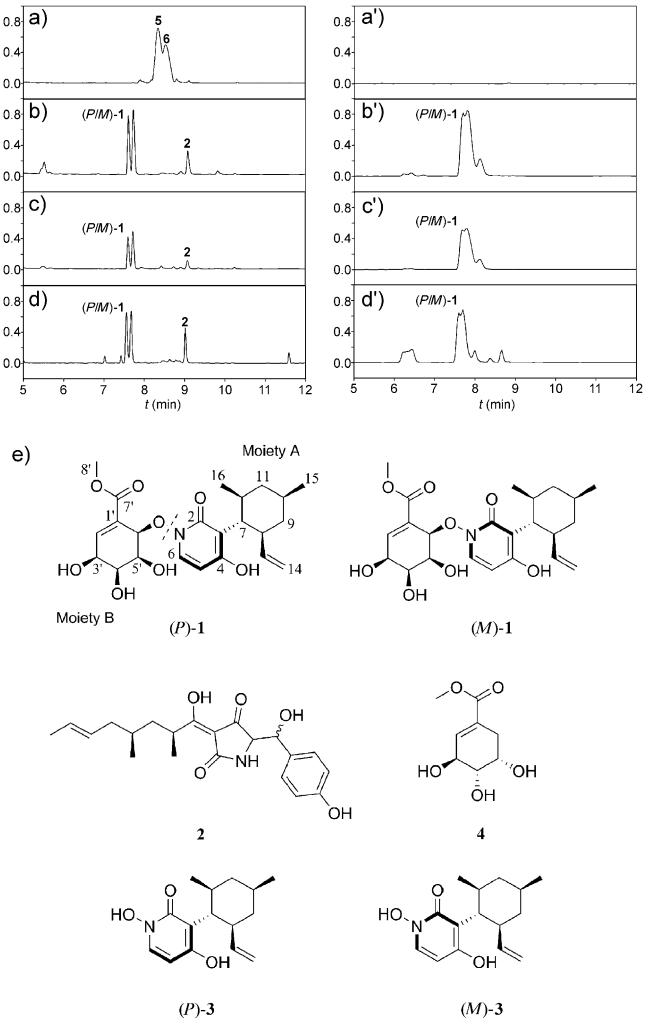

Figure 1. LC-MS profiling: chromatograms showing photodiode array data at 200–600 nm (a–d) and (+) ESI-MS selected ion traces at *m*/*z* 450 (a′–d′) of secondary metabolites produced by the *Tolypocladium* sp. isolate and structures of the indicated compounds (e). For the stacked spectra, the vertical axes show a normalized intensity scale. The fungus was cultured under the following conditions: PDB with $NaNO_3$ (a and a′), PDB with $NaNO_3$ and 5-azacytidine (b and b′), PDB (c and c′), co-culture with *Pseudomonas fulva* in PDB with $NaNO_3$ (d and d′).

ure 1 c,c′), or grown in PDB medium without $NaNO_3$ (Figure 1 d,d′), the production of peptides **5** and **6** was suppressed, and a new polyketide-shikimate-NRPS-hybrid metabolite, maximiscin [(*P*/*M*)-**1**], was obtained. These changes were accompanied by the production of (−)-methyl shikimate (**4**)[7] and the tetramic acid metabolite, F-14329 (**2**),[8] which appeared to have biosynthetic origins similar to (*P*/*M*)-**1**. Furthermore, when the fungus was treated with 5-azacytidine in PDB without $NaNO_3$, the biosynthesis of (*P*/*M*)-**1** was nearly suppressed, but the production of the polyketide-NRPS metabolite pyridoxatin was observed [(*P*/*M*)-**3**; Supporting Information, Figure S3].[9]

In solution, (*P*/*M*)-**1** was detected as an approximate 9:5 mixture of two rapidly interconverting atropisomers (Figure 1). The planar structures and relative configurations of moieties **A** and **B** in (*P*/*M*)-**1** were established by comprehensive analysis of the HRESIMS and 1D (^1H and ^{13}C) and 2D (^1H-^1H COSY, ^1H-^{13}C HSQC, ^1H-^{13}C HMBC, and ^1H-^1H ROESY) NMR data. Although no ^1H-^{13}C HMBC correlations were detected linking the two fragments, the downfield shift of C6′ ($\delta_C = 86.5$ ppm) relative to the carbasugar analogs (+/−)-pericosines B and C[10] ($\delta_C = 76$–ca.79 ppm) and a ^1H-^1H ROESY correlation between H6 and H6′, provided compelling evidence that the substructures were joined by a O=C-N-O-C bridge between moieties **A** and **B**. The O=C-N-O-C bridge in (*P*/*M*)-**1** is unusual among natural products; in contrast, similar N-O-C bridges have been described from a limited number of natural sources (such as the enediyne-antibiotic calicheamicins from *Micromonospora echinospora*).[11]

To further investigate the absolute configuration of the metabolite, a methanolic solution of (*P*/*M*)-**1** was mixed with $CuSO_4$ and subjected to stirring at room temperature for seven days.[12] Upon purification of the reaction mixture, blue crystals of a Cu(pyridoxatin)$_2$ chelate (**7**) together with a carbasugar product were obtained (Scheme 1). Single crystal X-ray diffraction analysis of the blue crystalline material revealed two organometallic complexes, (*P*,*M*)-**7** and (*P*,*P*)-**7**, co-located in the crystal lattice, which established the absolute configuration for this portion of the molecule as 7*R*,8*S*,10*R*,12*S*. Our data (Supporting Information, Page S8) for the carbasugar product **8** matched literature values reported for (+)-pericosine C.[10] In light of the relative

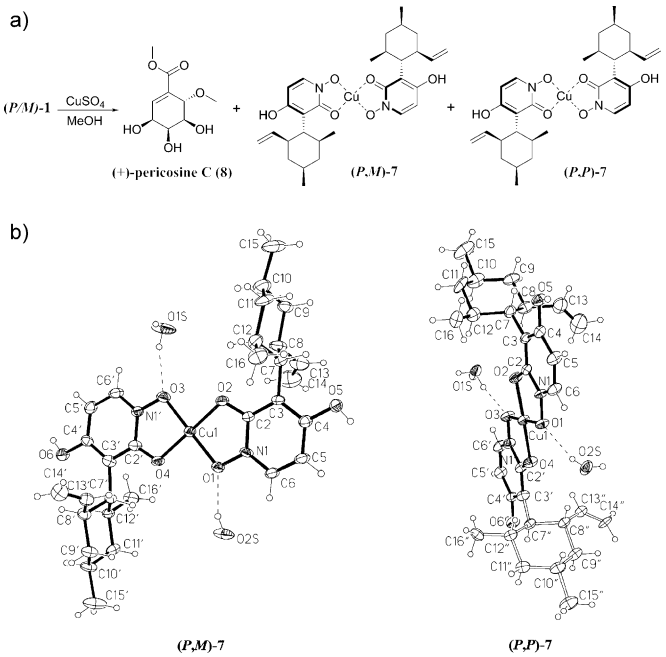

Scheme 1. a) O=C-N-O-C bridge cleavage reaction of (*P*/*M*)-**1** with $CuSO_4$ in MeOH. b) ORTEP structures generated from the X-ray diffraction data for a single crystal of **7**.

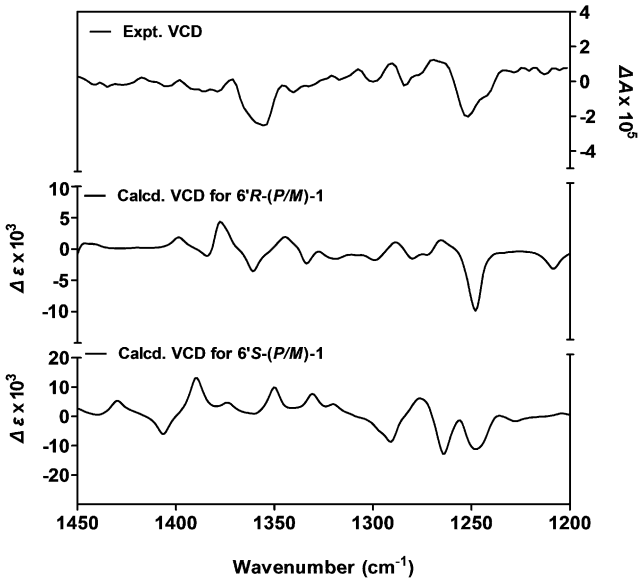

Figure 2. Comparison of the experimental VCD spectrum of (*P*/*M*)-**1** ([D_6]DMSO) with the calculated VCD spectra of 6′*R*-(*P*/*M*)-**1** and 6′*S*-(*P*/*M*)-**1**.

configuration we had proposed for the carbasugar in (*P*/*M*)-**1**, this result implied that the C6′ position underwent epimerization during methanolysis to yield a compound with a 3*S*,4*S*,5*S*,6*S* configuration (Scheme 1). The 6′*R* configuration of (*P*/*M*)-**1** was confirmed by comparison of the VCD spectrum (Figure 2) and specific rotation ($[\alpha]^{20}_{D}$ −147) of the metabolite with the theoretical VCD spectra (Figure 2) and the specific rotation of 6′*R*-(*P*/*M*)-**1** ($[\alpha]_D$ −94) and 6′*S*-(*P*/*M*)-**1** ($[\alpha]_D$ +151) generated by quantum chemical calculations (Tables S3 and S4). (*P*/*M*)-**1** exhibited strong VCD signals in the range of 1200–1450 cm^{-1} that matched well with the calculated VCD spectrum of the 6′*R*-(*P*/*M*)-**1** diastereomer (Figure 2). In contrast to previous VCD studies of stable atropisomers,[13] this application of VCD to an interconverting atropisomeric mixture required special consideration of the conformer populations attributable to both molecules in order to carry out predictive quantum chemical calculations.

To assign which sets of ^{1}H and ^{13}C NMR spins were attributable to each of the atropisomers, the ^{13}C NMR resonances for (*P*/*M*)-**1** were compared to values published for stable analogs, as well as data obtained from ab initio quantum chemical calculations. A well-defined trend was observed for the calculated differences between the ^{13}C NMR shifts of C2, C4, C8, and C12 for the *P* and *M* isomers of 1, pyridoxatin (**3**),[9] and cordypyridones A [(*P*)-**9**] and B[(*M*)-**9**],[14] which closely matched their respective published data sets (Figure S2). Applying this trend, we were able to assign the *P* and *M* atropisomers of (*P*/*M*)-**1** to their respective NMR data sets (Table S1).

Stable isotope labeling experiments with ^{13}C- and ^{15}N-enriched precursors were carried out on (*P*/*M*)-**1** using the substrates listed in Table S2. Feeding experiments employing [3-^{13}C]-D-glucose and [U-$^{13}C_6$]-D-glucose provided evidence that the carbasugar was derived from a shikimate pathway (Scheme 2; see also Figure S4).[15] Based on our studies, it is not certain if the stereocenters in the carbasugar are fixed early (route B) or late (route A) during the biosynthetic process (Scheme 2). Further supplementation of the culture medium with [1-^{13}C] sodium acetate and [2-^{13}C] sodium acetate enabled us to infer the likely polyketide origins of carbon atoms C2, C3, and C7 through C14 in (*P*/*M*)-**1** (Scheme 2; see also Table S2). Although the biosynthetic pathways of related tetramic acids and 5-phenyl-pyridones have been investigated,[16] the NRPS origins of C4, C5, C6 and N1 in 5-*H*-pyridones (for example, pyridoxatin, PF1140, *N*-deoxy-PF1140, and related compounds) had not been unequivocally defined. Considering the related structural features of (*P*/*M*)-**1** and F-14329 (**2**),[8] we speculated that tyrosine could serve as the preferred or only substrate utilized in the biosynthesis of related 5-*H*-pyridones. To test this, [1-^{13}C]-L-tyrosine and [^{15}N]-L-tyrosine were added to the fungal culture, resulting in isotope incorporation at positions C4 (an enrichment factor of 11.8; Table S2) and N1 (Figure S33) of (*P*/*M*)-**1**, respectively. Moreover, we observed that [U-$^{13}C_6$]-D-glucose feeding led to the contiguous ^{13}C-enrichment of C4, C5, and C6 (Table S2), as anticipated for the catabolic/anabolic transformation of glucose into tyrosine (Scheme 2; see also Figure S4). These data provided evidence for the direct incorporation of tyrosine into (*P*/*M*)-**1**, which was then biotransformed by the fungus to remove the phenol moiety. The proposed pathway for the formation of (*P*/*M*)-**1** provides a compelling rationale for how other *N*-hydroxy-pyridone-containing natural products may be generated through a parallel biosynthetic process. In light of the unique mixed biosynthetic origins of (*P*/*M*)-**1**, we have given this metabolite the colloquial name maximiscin, based loosely on a combination of the Latin words *maximopere* (meaning very or exceedingly) and *miscellus* (meaning blended).

The antiproliferative and cytotoxic activities of (*P*/*M*)-**1** were tested in an NCI-60 in vitro cell panel. Compound (*P*/*M*)-**1** exhibited antiproliferative activity against several cell lines, with an average GI_{50} value of 0.39 μM (Table S6). Closer examination of these data revealed that the UACC-62 melanoma cell line was not only sensitive to (*P*/*M*)-**1** (LC_{50} = 0.93 μM), but it also exhibited a monophasic dose-response curve (Figure S29 A) that was dissimilar to the biphasic dose-response curves exhibited by most of the other cell lines. For example, the dose-response curves for (*P*/*M*)-**1** against both MDA-MB-453 and HeLa cell lines were biphasic (Figure S29 A), which indicates the possibility of two separate mechanisms of action. Although this response pattern was robust and fully reproducible, further studies will be required to elucidate the specific mechanisms of action of (*P*/*M*)-**1** in these different cell lines.

A common mechanism of drug resistance exhibited by cancer cells is expression of Pgp (a product of the *MDR1* gene), which contributes to the efflux of drugs and toxic substrates.[17] To determine if (*P*/*M*)-**1** can overcome Pgp-mediated resistance, the compound was evaluated in a SK-OV-3/MDR-1-6/6 ovarian cancer cell line transduced with Pgp[18] and compared to the untransformed parent SK-OV-3 cell line. The SK-OV-3/MDR-1-6/6 cell line demonstrated substantial resistance to the antiproliferative effects of PTX (Figure 3). In contrast, (*P*/*M*)-**1** exhibited equivalent inhib-

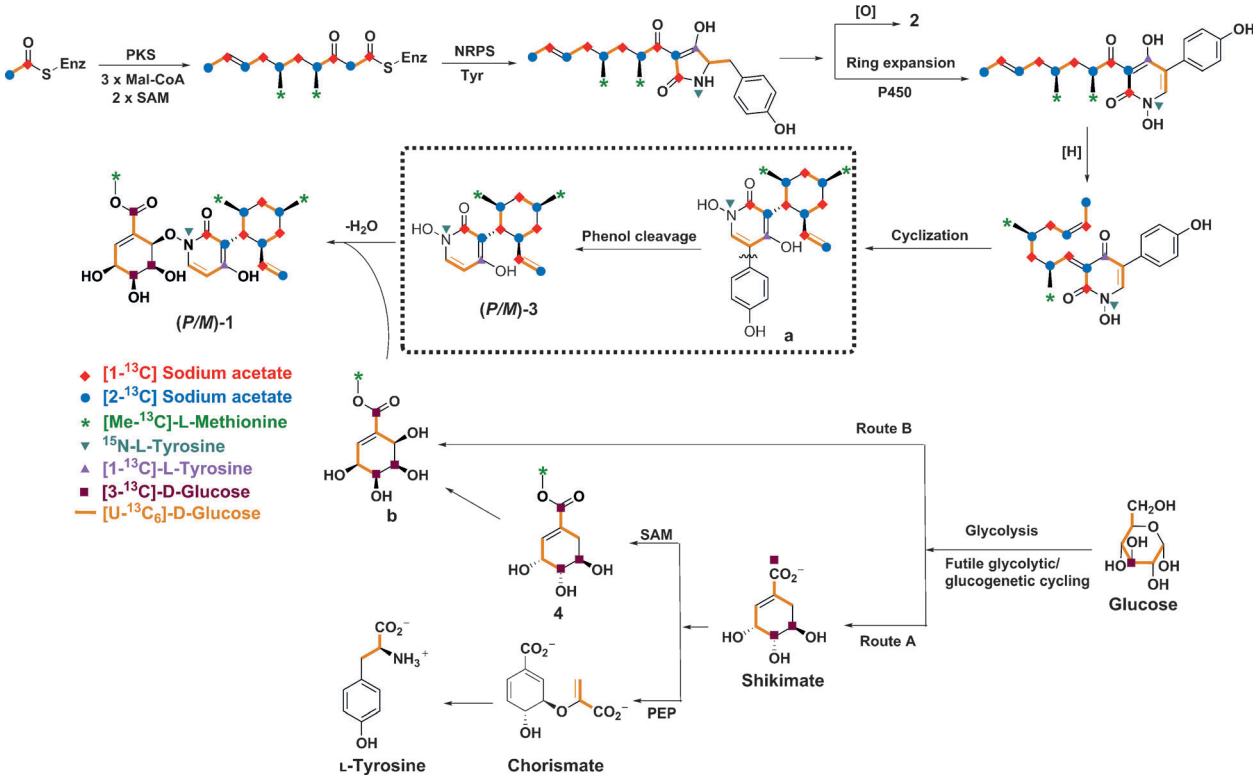

Scheme 2. Proposed biogenetic pathway for (*P*/*M*)-**1** established on the basis of stable isotope incorporation patterns for (*P*/*M*)-**1** generated by feeding experiments with the *Tolypocladium* sp. isolate using [1-^{13}C] sodium acetate, [2-^{13}C] sodium acetate, [Me-^{13}C]-L-methionine, [1-^{13}C]-L-tyrosine, [^{15}N]-L-tyrosine, [3-^{13}C]-D-glucose, and [U-^{13}C$_6$]-D-glucose.

itory activities against both cell lines, which suggests that it is not a substrate for Pgp (Figure 3).

Based on the potency and monophasic dose-response pattern of (*P*/*M*)-**1** against the UACC-62 cells, this cell line was chosen for further studies. A clonogenic assay was performed to determine the capacity of (*P*/*M*)-**1** to inhibit colony formation and the persistence of its cellular effects in UACC-62 cells. Cells were treated with (*P*/*M*)-**1** for 8 h, after which the compound was removed by washing the cells. Treatment at a concentration of 6 μM resulted in a significant decrease in colony formation ($p \leq 0.01$) compared to vehicle-treated controls (Figure 4). These results indicate that, subsequent to drug removal, the biological effects of (*P*/*M*)-**1** against UACC-62 cells are moderately persistent.

With these promising results, we proceeded to investigate whether (*P*/*M*)-**1** had antitumor activity in vivo by evaluating its activity in a UACC-62 xenograft mouse model. Athymic

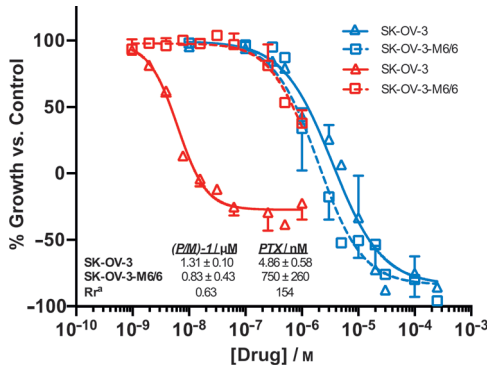

Figure 3. Dose-response curves for growth inhibition of SK-OV-3 and SK-OV-3-M6/6 cells after 48 h of treatment with (*P*/*M*)-**1** or paclitaxel (PTX). Data points represent the mean standard error for three independent experiments, performed in triplicate. Error bars, when not visible, are within the boundaries of the data points. GI_{50} values represent the mean standard deviation for three independent experiments, performed in triplicate. Percent growth was calculated as previously described.[19] Relative resistance (^{a}Rr) values were calculated as: [(GI_{50} in SK-OV-3 M6/6 cells)/(GI_{50} in SK-OV-3 cells)].

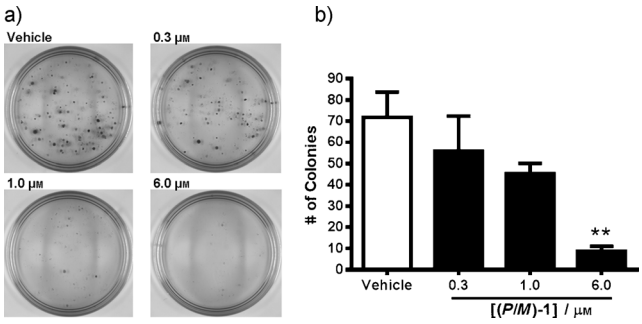

Figure 4. Clonogenic assay results for UACC-62 cells after 8 h of exposure to (*P*/*M*)-**1** at the indicated concentrations. a) Representative images of UACC-62 cell colonies after 14 days of growth and crystal violet staining. b) Quantification of mean colony numbers for three independent experiments, performed in duplicate or triplicate. Error bars indicate the standard deviation. $^{**}P < 0.01$ compared to vehicle; one-way ANOVA with Dunnett's post-hoc test.

nude mice bearing UACC-62 xenograft tumors were treated by administering (*P*/*M*)-**1** (5 mg kg^{-1}) daily for 5 d, withholding treatment for 2 d, and then providing daily treatment with (*P*/*M*)-**1** (5 mg kg^{-1}) for an additional 5 d. This dosing schedule provided significant inhibition of tumor growth relative to untreated control mice ($p = 0.027$; Figure 5) without causing substantial weight loss (Figure S29). The UACC-62 cell line forms an aggressive, rapid-growing tumor in vivo, so the experiment was discontinued after 14 d due to excessive tumor burden in the control mice.

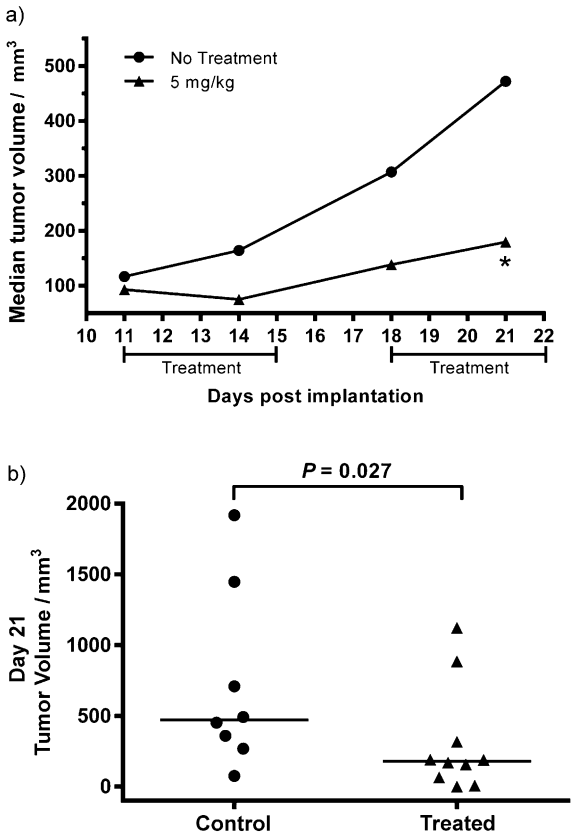

Figure 5. Inhibition of UACC-62 xenograft tumor growth in nude mice by (***P*/*M***)-**1**. a) Growth curves showing the median tumor volume ($n = 8$–10 tumors per group). Mice were dosed daily during the indicated treatment periods. *$P = 0.027$ compared to untreated control mice by the Mann–Whitney *U* test. b) Comparison of tumor volumes at 21 days after tumor implantation.

In summary, a new *Tolypocladium* sp. isolate was obtained through our crowdsourcing initiative. This isolate produced the unique polyketide-shikimate-NRPS-hybrid compound (*P*/*M*)-**1** via chemical epigenetic induction, culture medium variation, and bacterial co-culture strategies. The results of these studies speak to the multitude of interdependent factors involved in stimulating fungal secondary metabolite biosynthesis. Compound (*P*/*M*)-**1**, which possesses an unusual O=C-N-O-C bridge, showed in vitro cytotoxic activity against a number of cell types and in vivo antitumor activity in a UACC-62 xenograft cancer model. Moreover, (*P*/*M*)-**1** exhibited an ability to circumvent Pgp-mediated drug resistance, which makes this a potentially valuable compound for further investigation. These results also highlight the remarkable opportunities that exist for fostering the meaningful involvement of citizen scientists in research programs, and how their participation can substantially enhance scientific investigations.

Received: July 26, 2013
Revised: September 26, 2013
Published online: November 27, 2013

Keywords: antitumor agents · biosynthesis · crowdsourcing · drug discovery · epigenetics

[1] a) N. A. Kartsonis, J. Nielsen, C. M. Douglas, *Drug Resist. Updates* **2003**, *6*, 197–218; b) N. Kardos, A. L. Demain, *Appl. Microbiol. Biotechnol.* **2011**, *92*, 677–687; c) A. Endo, *Proc. Jpn. Acad. Ser. B* **2010**, *86*, 484–493.

[2] a) M. Stadler, N. P. Keller, *Mycol. Res.* **2008**, *112*, 127–130; b) L. W. Wang, Y. L. Zhang, F. C. Lin, Y. Z. Hu, C. L. Zhang, *Mini. Rev. Med. Chem.* **2011**, *11*, 1056–1074; c) M. E. Rateb, R. Ebel, *Nat. Prod. Rep.* **2011**, *28*, 290–344.

[3] D. L. Hawksworth, *Stud. Mycol.* **2004**, 9–17.

[4] Natural Product Discovery Group Home Page. http://npdg.ou.edu/citizenscience (accessed May 14, **2013**).

[5] a) Grímsvötn 2011 Ash Collection Findings Web Page. http://www.bgs.ac.uk/discoveringGeology/hazards/volcanoes/grimsvotn2011.html (accessed May 14, **2013**); b) T. Gura, *Nature* **2013**, *496*, 259–261; c) C. Lintott, K. Schawinski, S. Bamford, A. Slosar, K. Land, D. Thomas, E. Edmondson, K. Masters, R. C. Nichol, M. J. Raddick, A. Szalay, D. Andreescu, P. Murray, J. Vandenberg, *Mon. Not. R. Astron. Soc.* **2011**, *410*, 166–178; d) R. M. Merchant, D. A. Asch, J. C. Hershey, H. M. Griffis, S. Hill, O. Saynisch, A. C. Leung, J. M. Asch, K. Lozada, L. D. Nadkarni, A. Kilaru, C. C. Branas, E. M. Stone, L. Starr, F. Shofer, G. Nichol, L. B. Becker, *Circ. Cardiovasc. Qual. Outcomes.* **2013**, *6*, 229–236; e) The CornellLab of Ornithology-Citizen Science Central Web Page. http://www.birds.cornell.edu/citscitoolkit (accessed May 14, **2013**).

[6] a) X. R. Wang, J. L. You, J. B. King, D. R. Powell, R. H. Cichewicz, *J. Nat. Prod.* **2012**, *75*, 707–715; b) L. Du, J. B. King, B. H. Morrow. , J. K. Shen, A. N. Miller, R. H. Cichewicz, *J. Nat. Prod.* **2012**, *75*, 1819–1823.

[7] N. Armesto, S. Fernandez, M. Ferrero, V. Gotor, *Tetrahedron* **2006**, *62*, 5401–5410.

[8] N. Takashi, N. Mutsuo, K. Hidetake, T. Masaaki, T. Isshin, In *Jpn. Kokai Tokkyo Koho*, Vol. JP 2007153840 A 20070621, **2007**.

[9] Y. Teshima, K. Shin-ya, A. Shimazu, K. Furihata, H. S. Chul, K. Furihata, Y. Hayakawa, K. Nagai, H. Seto, *J. Antibiot.* **1991**, *44*, 685–687.

[10] a) T. Yamada, M. Iritani, H. Ohishi, K. Tanaka, K. Minoura, M. Doi, A. Numata, *Org. Biomol. Chem.* **2007**, *5*, 3979–3986; b) Y. S. Reddy, P. Kadigachalam, R. K. Basak, A. P. J. Pal, Y. D. Vankar, *Tetrahedron Lett.* **2012**, *53*, 132–136; c) Y. Usami, M. Ohsugi, K. Mizuki, H. Ichikawa, M. Arimoto, *Org. lett.* **2009**, *11*, 2699–2701; d) Y. Usami, Y. Ueda, *Synthesis* **2007**, 3219–3225.

[11] M. D. Lee, J. K. Manning, D. R. Williams, N. A. Kuck, R. T. Testa, D. B. Borders, *J. Antibiot.* **1989**, *42*, 1070–1087.

[12] N. Momiyama, H. Yamamoto, *J. Am. Chem. Soc.* **2003**, *125*, 6038–6039.

[13] a) R. H. Cichewicz, L. J. Clifford, P. R. Lassen, X. Cao, T. B. Freedman, L. A. Nafie, J. D. Deschamps, V. A. Kenyon, J. R. Flanary, T. R. Holman, P. Crews, *Bioorg. Med. Chem.* **2005**, *13*, 5600–5612; b) T. B. Freedman, X. Cao, L. A. Nafie, M. Kalber-

matter, A. Linden, A. J. Ripper, *Helv. Chim. Acta* **2005**, *88*, 2302 – 2314.
[14] M. Isaka, M. Tanticharoen, P. Kongsaeree, Y. Thebtaranonth, *J. Org. Chem.* **2001**, *66*, 4803 – 4808.
[15] R. Bentley, *Crit. Rev. Biochem. Mol. Biol.* **1990**, *25*, 307 – 384.
[16] D. Boettger, C. Hertweck, *ChemBioChem* **2013**, *14*, 28 – 42.
[17] S. Nobili, I. Landini, T. Mazzei, E. Mini, *Med. Res. Rev.* **2012**, *32*, 1220 – 1262.
[18] D. Sadava, A. Coleman, S. E. Kane, *J. Liposome Res.* **2002**, *12*, 301 – 309.
[19] M. R. Boyd, K. D. Paull, L. R. Rubinstein, *Cytotoxic Anticancer Drugs: Models and Concepts for Drug Discovery and Development* (Eds: F. A. Valeriote, T. Corbett, L. Baker), Kluwer, Dordrecht, **1992**, pp. 1134.

